Advances in Agriculture, Sciences and Engineering Research
http://www.ejournal.sedinst.com
© Science Education Development Institute, 2013 **Volume 3 (7) July: 972 - 983, 2013**
Printed in Nigeria **ISSN: 2276 – 6723**

HEAT AND HALL EFFECT OF AN OSCILLATING PLATE IN A POROUS MEDIUM

A. M. Okedoye
Department of Mathematics, Covenant University Km. 10, Idiroko Road, P. M. B. 1023, Ota, Ogun State, (NIGERIA). E – mail: dele.okedoye@covenantuniversity.edu.ng, micindex@yahoo.com.

ABSTRACT
An exact solution of the flow of heat and viscous fluid on a porous plate by using perturbation is obtained for the conjugate problem of an electrically conducting fluid in the presence of strong magnetic field by introducing the Hall currents. The fluid half-space is considered to be porous. Large time solution and effects of porous medium are discussed. It was shown that Hall Effect setup an opposing force which reduces the velocity. Temperature and velocity distributions have been obtained and the effect of various values of nondimensional physical parameters on streamline patterns and skin friction coefficient and Nusselt number are presented and discussed.

KEYWORDS: Stokes problem, Porous medium, Hall effects, Heat transfer, Electrically conducting fluid.
Mathematics Subject Classification: 76W05, 76D05, 80A20

INTRODUCTION

Hall effect is commonly used in distributors for ignition timing (and in some types of crank and camshaft position sensors for injection pulse timing, speed sensing, etc.) the Hall effect sensor is used as a direct replacement for the mechanical breaker points used in earlier automotive applications in Automotive ignition and fuel injection. Fluid dynamics and heat transfer process associated with cooling of an accelerating flat surface has considerable practical importance as pointed out by Crane [1], Chakraborty and Gupta [2], and Dutta and Gupta [3].

Newton introduced the concept of "lack of slipperness" which is important quantity that we call viscosity. Navier, in 1827 [4], derived the Navier-Stokes equation but he did not attach much physical significance to viscosity. Stokes gave the correct form to the constitutive equation that we call a Newtonian fluid. Stokes' first problem, also known as Rayleigh's problem [5], was solved by Stokes in 1851 [6]. The unsteady flow problem studies the diffusion of vorticity in a half space filled with a Newtonian, incompressible fluid which moves when an infinite plate starts a constant velocity parallel to itself (in its own plane) from rest position. Stokes second problem [6] also defines the same geometry except the case that the infinite plate starts oscillations with $u_w \cos \omega t$.

In recent years the theoretical study of magnetohydrodynamics (MHD) channel flows has been a subject of great interest due to its widespread applications in designing cooling systems with liquid metals, petroleum industry, purification of crude oil, polymer technology, centrifugal separation of matter from fluid, MHD generators, pumps, accelerators and flow meters [5, 7]. Unfortunately, the results of these investigations cannot be applied to the flow of ionized gases. In an ionized gas where the density is low and/or the magnetic field is very strong, the conductivity normal to the magnetic field is reduced due to the free spiraling of electrons and ions about the magnetic lines of force before severing collisions; also, a current is induced in a direction normal to both the electric and magnetic fields. The phenomena, well known in the literature, are called the Hall Effect [6, 8, 9]. The study of magnetohydrodynamic flows with Hall currents has important engineering applications in problems of magnetohydrodynamic generators and of Hall accelerators as well as in flight magnetohydrodynamics.

NOMENCLATURE

A_1	Rivlin-Ericksen tensor			C_p	specific heat
B	magnetic field			$Q_{0'}$	Heat source/Sink parameter
B_0	applied magnetic field			∇	nabla/del operator
E	electric field current			$i=\sqrt{-1}$	complex identity
e	electron charge			**Greek letters**	
$grad$	gradient operator			β_1	plate acceleration parameter
J	current density			μ	dynamic viscosity
K	constant permeability			μ_m	magnetic permeability
M	MHD parameter			υ	kinematic viscosity
η_e	number density of electrons			ρ	fluid density
p	scalar pressure			σ	electrical conductivity
p_e	electron pressure			τ_e	electron collision time
t	Time			τ_i	ions collision time
T_c	Cauchy stress tensor			φ	porosity parameter
u_w	main stream velocity/free stream			ϕ	Hall parameter
u , v	velocity components			q_i	cyclotron frequency of ions
V	velocity vector			ω_e	cyclotron frequency of electrons
v_w	suction/blowing velocity			ω	oscillating frequency
x , y	coordinate axis				

The study of magnetohydrodynamic flows with Hall currents has important engineering applications in problems of magnetohydrodynamic generators and of Hall accelerators as well as in flight magnetohydrodynamics. Effects of Hall current and heat transfer on flow due to a pull of eccentric rotating disks was investigated by Asghar *et al*.[10]. They reported that when the magnetic Reynolds number is very small, the flow pattern with Hall effects is remarkably similar to that for non-conducting flow. Of course, the assumption of very small magnetic Reynolds number will be valid for flow of liquid metals or slightly ionized gas. Guria *et.al.* [11] present an exact solution of the unsteady hydromagnetic flow due to non-coaxial rotations of a porous disk and a fluid at infinity is taking Hall currents into account. An analytical solution of the problem is obtained for small and large times after the start by the Laplace transform method. It is found that for small values of time there is no inertial oscillation while for large time the steady state is reached through inertial oscillations. The frequency of these oscillations first increases reaches a maximum and then decreases with increase in Hall parameter. Mohammadreza*et. al*. [12] presents the study of momentum characteristics in a MHDviscous flow over a stretching sheet. The analytical method called Differential Transformation Method (DTM) powered by the Pade' approximation is was applied to solve the nonlinear equation derived from MHD viscous flow over a stretching sheet, The obtained results approve its efficiencies and capabilities beside numerical solutions achieve.

Hall Effect devices when appropriately packaged are immune to dust, dirt, mud, and water. These characteristics make Hall Effect devices better for position sensing than alternative means such as optical and

electromechanical sensing. Hall Effect sensors may be used in various sensors such as rotating speed sensors (bicycle wheels, gear-teeth, automotive speedometers, electronic ignition systems), fluid flow sensors, current sensors, and pressure sensors. Common applications are often found where a robust and contactless switch or potentiometer is required. These include: electric airsoft guns, triggers of electropneumatic paintball guns, go-cart speed controls, smart phones, and some global positioning systems.

The present investigation aims at obtaining the analytical solution of coupled heat and mass transfer equations in the half-space of the Stokes' problem with a porous half space of constant permeability ($K > 0$) and porosity ($\varphi > 0$) and discussed the influence of Hall current on the MHD flow. The infinite plate at $y = 0$ starts oscillations with the velocity $u_w e^{(\beta_1 - i\omega)t}$, for $t > 0$. Darcy's law was used to incorporate the effects of pores on the velocity field [13].

Formulation of the basic equations

Consider the unsteady flow of an incompressible viscous fluid past an accelerating vertical porous plate. Let the x-axis be directed upward along the plate and the y-axis normal to the plate. Let u and v be the velocity components along the x- and y- axes respectively. Let us assume that the plate is accelerating with a velocity $u_w e^{(\beta_1 - i\omega)t}$ in its own plane. The MHD equations governing the unsteady flow of an incompressible fluid together with Brinkman's empirical modification of Darcy's law are

$$\nabla \cdot V = 0 \tag{2.1}$$

$$\rho\left(\frac{\partial V}{\partial t} + (V \cdot \nabla)V\right) = -\nabla p + \nabla T_c + J \wedge B \tag{2.2}$$

$$\nabla \cdot B = 0,\ \nabla \wedge B = \mu_m J,\ \nabla \wedge E = 0 \tag{2.3}$$

$$\rho c_p\left(\frac{\partial T}{\partial t} + (V \cdot \nabla)T\right) = \alpha \nabla^2 T + (T - T_\infty)Q_0 \tag{2.4}$$

Making reference to Cowling [14], when the strength of the magnetic field is very large, the generalized Ohm's law is modified to include the Hall current so that

$$J + \frac{\omega_e \tau_e}{B_0}(J \wedge B) = \sigma\left(E + V \wedge B + \frac{1}{en_e}\nabla p_e\right) \tag{2.5}$$

The ion-slip and thermoelectric effects are not included in (2.5). Further, it is assumed $\omega_e \tau_e \approx O(1)$ and $\omega_i \tau_i << 1$, where ω_i and τ_i are the cyclotron frequency and collision time for ions respectively. Under these assumptions Eq. (2.5) with the help of equations (2.3) and (2.5) becomes [15]

$$J \wedge B = -\frac{\sigma B_0^2 (1 + i\phi)}{1 + \phi^2} \tag{2.6}$$

We have also assumed that the flow is confined $(y > 0)$ in a porous medium with constant permeability $K(> 0)$ and porosity $\varphi(\varphi > 0)$ [10]

$$\nabla p = -\frac{\mu \varphi}{K} V \tag{2.7}$$

In equation (2.2) $T_c = \mu A_1$ (in which A_1 is the first Rivlin-Ericksen tensor). A_1 is defined by

$$A_1 = L + L^T,\ L = \nabla V \tag{2.8}$$

where L is the gradient of velocity field and L^T is the transpose of the gradient of velocity field. On substituting equations (2.6) – (2.8), we have

$$\rho\left(\frac{\partial V}{\partial t}+(V\cdot\nabla)V\right)=-\frac{\mu\varphi}{K}V+\mu\nabla^2V-\frac{\sigma B_0^2}{1-i\phi}V+g\beta(T-T_\infty) \tag{2.9}$$

On disregarding the Joulean heat dissipation, the boundary conditions are given by

$$\left.\begin{array}{c} u=0,\ \ T=T_\infty,\ \ for\ all\ \ y,\ t\le 0 \\ u=u_we^{(\beta_1-i\omega)t},\ v=-v_w,\ T=T_w+\varepsilon e^{(\beta_1-i\omega)t},\ \ y=0,\ t>0 \\ u=0,\ T=T_\infty,\ \ as\ \ y\to\infty,\ t>0 \end{array}\right\} \tag{2.10}$$

We consider the fluid lying in the upper half space/plane. The $x-$ axis is taken along the flow direction and $y-$ axis perpendicular to it: such that there is simultaneous suction/blowing at the boundary $y = 0$. In fact, it follows from the continuity equation (2.1) that

$$\frac{\partial v}{\partial y}=0 \tag{2.11}$$

which implies $v=-v_w=const$

so that the velocity field takes the form

$$V=(u(y,t),v_w) \tag{2.12}$$

Let us introduce the non-dimensional variables

$$u'=\frac{u}{u_w},\ t'=\frac{tv_w^2}{\upsilon},\ y'=\frac{yv_w}{\upsilon},\ \theta=\frac{T-T_\infty}{T_w-T_\infty} \tag{2.13}$$

where all the physical variables have their usual meanings.

With the help of (2.4), (2.9), (2.11), (2.12) and (2.13), on dropping primes ($'$) the governing equations with the boundary conditions (2.10) reduce to

$$\frac{\partial u}{\partial t}-\frac{\partial u}{\partial y}=\frac{\partial^2u}{\partial y^2}-\left(\lambda+\frac{M^2}{1-i\phi}\right)u+Grt\,\theta$$

(2.14)

$$\Pr\left(\frac{\partial\theta}{\partial t}-\frac{\partial\theta}{\partial y}\right)=\frac{\partial^2\theta}{\partial y^2}+\Pr\beta\theta \tag{2.15}$$

$$\left.\begin{array}{c} u=0,\ \ \theta=0,\ \ \ for\ all\ \ y,\ \ t\le 0 \\ u=e^{(\beta_1-i\omega)t},\ \theta=1+\varepsilon e^{(\beta_1-i\omega)t},\ y=0,\ t>0 \\ u\to 0,\theta\to 0,as\ y\to\infty,\ \ t>0 \end{array}\right\} \tag{2.16}$$

Where the parameters are as defined below:

$$Gr\tau=\frac{g\beta_\tau(T_w-T_\infty)\nu}{\rho v_w^3},\ \ M=\frac{\sigma B_0^2\upsilon}{\rho v_w^2},\ \Pr=\frac{\mu c_p}{\alpha},\ \ \beta=\frac{Q\mu\upsilon}{\alpha_0v_w^2\rho},\lambda=\frac{\upsilon^2\varphi}{v_w^2K}$$

where Pr, Grt, λ , β and M are Prandtl number, Grashof number for heat transfer, Porosity parameter, heat generation/absorption and Hartmann's number respectively.

Method of Solution

To solve the problem posed in equations (2.14) – (2.17), we seek a perturbation series expansion in the limit of ε for our dependent variables. This is justified since ε is small. Thus we write

$$\left.\begin{aligned} u(y,t) &= u_0(y) + \varepsilon e^{(\beta_1 - i\omega)t} u_1(y) + o(\varepsilon^2) + \ldots. \\ \theta(y,t) &= \theta_0(y) + \varepsilon e^{(\beta_1 - i\omega)t} \theta_1(y) + o(\varepsilon^2) + \ldots. \end{aligned}\right\} \tag{3.1}$$

The use of perturbation technique therefore has an advantage over Fourier transform method as $\theta_i(y)$ and $u_i(y)$ is zero for $i \geq 2$ that is, the actual solutions are as stated in equation (3.1). So for the problem addressed here, perturbation approximate solutions do provide adequate answers.

Substituting equations (2.14) and (2.17) and the expression for the stream into equations (3.1), equating the harmonic and non – harmonic terms and neglecting the coefficient of ε^2, we obtain the equations governing the steady state motion and the equations governing the transient.

$$\frac{d^2\theta_0}{dy^2} + \Pr\frac{d\theta_0}{dy} - \Pr\beta\theta_0 = 0 \tag{3.2}$$

$$\theta_0(0) = 1,\ \theta_0(y) \to 0 \ \ as\ y \to \infty$$

$$\frac{d^2u_0}{dy^2} + \frac{du_0}{dy} - \left(\frac{M^2}{1 - i\phi} + \lambda\right)u_0 = -Gr\,\tau\theta_0 \tag{3.3}$$

$$u_0(y) = e^{(\beta_1 - i\omega)t} \ \ at\ y = 0,\ \ u_0(y) \to 0 \ \ \ as\ y \to \infty$$

and

$$\frac{d^2\theta_1}{dy^2} + \Pr\frac{d\theta_1}{dy} - \Pr(\beta - \beta_1 + i\omega)\theta_1 = 0 \tag{3.4}$$

$$\theta_1(y) = e^{(\beta_1 - i\omega)t}\ at\ y = 0,\ \ \theta_1(y) \to 0\ \ as\ y \to \infty$$

$$\frac{d^2u_1}{dy^2} + \frac{du_1}{dy} - \left(\frac{M^2}{1 - i\phi} + \lambda + \beta_1 - i\omega\right)u_1 = -Gr\,\tau\theta_1 \tag{3.5}$$

$$u_1(y) = 0\ \ at\ y = 0,\ \ u_1(y) \to 0 \ \ \ as\ y \to \infty$$

These sets of equations are now solved analytically for the velocity and the temperature fields. The solutions of equations (3.2) – (3.5) are

$$\begin{aligned} &\theta_0(y) = e^{-ny},\ \ u_0(y) = a_2 e^{-my} + a_3 e^{-ny} \\ &\theta_1(y) = e^{-n_1 y},\ \ u_1(y) = a_6 e^{-m_1 y} + a_7 e^{-n_1 y} \end{aligned} \tag{3.6}$$

where

$$n = \frac{1}{2}\left(\Pr + \sqrt{\mathbf{Pr}^2 - 4\mathbf{P}r\beta}\right),\ \ n_1 = \frac{1}{2}\left(\Pr + \sqrt{\Pr^2 - 4\Pr(\beta - \beta_1 + i\omega)}\right),$$

$$m = \frac{1}{2}\left(1 + \sqrt{1 + 4\left(\lambda + \frac{M^2}{1 - i\phi}\right)}\right),\ m_1 = \frac{1}{2}\left(1 + \sqrt{1 + 4\left(\lambda + \frac{M^2}{1 - i\phi} + \beta_1 - i\omega\right)}\right),$$

with $$a_2 = e^{(\beta_1 - i\omega)t} - a_3,\ a_6 = -a_7,$$

$$a_3 = \frac{-Grt}{n^2 - n - \left(\lambda + \frac{M^2}{1 - i\phi}\right)},\ a_7 = \frac{-Grt}{n_1^2 - n_1 - \left(\lambda + \frac{M^2}{1 - i\phi} + \beta_1 - i\omega\right)},$$

The functions $u_0(y)$ and $\theta_0(y)$ are the mean velocity and the mean temperature fields respectively; and $u_1(y)$ and $\theta_1(y)$ are, respectively, the velocity oscillatory part and the temperature oscillatory part fields.

Now substituting equations (3.8) into equation (3.1), we obtain the required expressions for velocity, temperature and magnetic induction;

$$\theta(y,t) = e^{-ny} + \varepsilon e^{(\beta_1 - i\omega)t} e^{-n_1 y} \tag{3.7}$$

$$u(y,t) = a_2 e^{-my} + a_3 e^{-ny} + \varepsilon e^{(\beta_1 - i\omega)t}\left(a_6 e^{-m_1 y} + a_7 e^{-n_1 y}\right) \tag{3.8}$$

The graphical representations of equations (3.7) and (3.8) are presented and analyse in section 4 of this work.

The parameters of engineering interest for the present problem are the local skin-friction coefficient (c_f) and the local Nusselt number (Nu) which are defined respectively by the following expressions:

Skin-Friction:We now study skin-friction from velocity field. It is given by

$$c_f = \frac{T_f}{\rho u_\omega v_\omega} = \frac{d^2}{dy^2} u(y,t)\Big|_{y=0}, \quad \tau_f = \mu \frac{du}{dy}\Big|_{y=0}$$

which reduces to

$$c_f = \left(\frac{\partial u}{\partial y}\right)_{y=0}$$

Therefore from equation (3.8)

$$c_f = -a_2 m - a_3 n - \varepsilon e^{(\beta_1 - i\omega)t}\left(a_6 m_1 + a_7 n_1\right)$$

Nusselt Number: In non-dimensional form, the rate of heat transfer at the wall is computed from Fourier's law and is given by

$$Nu = \frac{q_\omega v}{(T_\omega - T_\infty) K v_\omega} = \frac{-d}{dy}\theta(yt)\Big|_{y=0}, \quad q_\omega = -K \frac{dT}{dy}\Big|_{y=0},$$

Therefore from equation (3.7)

$$Nu = n + \varepsilon e^{(\beta_1 - i\omega)t} n_1$$

DISCUSSION OF RESULTS

The solution given in (3.7) and (3.8) are general (describing the combined effects of heat generation/absorption, porosity parameter, MHD parameter, Hall parameter, thermal Grashof number and acceleration/deceleration) and is independent of the form of the steady solution. For large times, we must recover the steady state solution. Indeed when t goes to infinity we have

$$\lim_{t\to\infty} e^{(\beta_1 - i\omega)t} \to \begin{cases} 0, & \beta_1 < 0 \\ \infty, & \beta_1 > 0 \end{cases} \tag{3.9}$$

thus one can easily obtain from (3.7) and (3.8)

$$\theta_{ss}(y) = e^{-ny},$$

$$u_{ss}(y) = a_2 e^{-my} + a_3 e^{-ny}$$

where $u_{ss}(y)$ and $\theta_{ss}(y)$ are the steady state solutions for heat and mass transfer. It is found from (3.9) that the solutions (3.7) and (3.8) are unbounded for acceleration that is when β is positive $(\beta_1 > 0)$, and remains bounded or convergent when is negative $(\beta_1 < 0)$.

In order to point out the effects of various parameters on the flow characteristic, the following considerations are made: To be realistic, the values of Prandtl number are chosen to be Pr=0.71 which represents air and Pr=0.015 for mercury at temperature 25°C and one atmospheric pressure. Attention is focused on positive values of the buoyancy parameters i.e. thermal Grashof number $Gr\tau > 0$ (which corresponds to the cooling problem).

The cooling problem is often encountered in engineering applications; for example in the cooling of electronic components and nuclear reactors. The effect of thermal Grashof number on velocity distribution is shown in Fig. 1. It is seen that velocity increases as thermal Grashof number increases with the highest amplitude close to the plate. Far away from the plate, damping occurs and the presences of peaks in the profile indicate that maximum velocity occurs in the body of the fluid close to the surface. A study of the curves of the Figure 1 shows that the Grashof number for thermal transfer accelerates the velocity of the flow field.

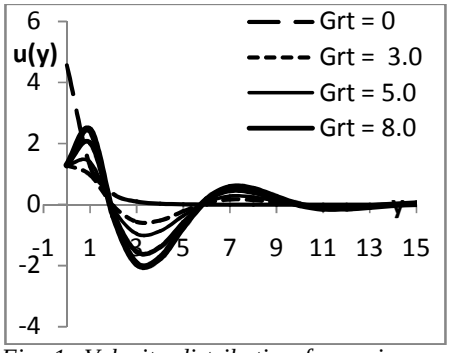

Fig. 1: Velocity distribution for various values of Grt

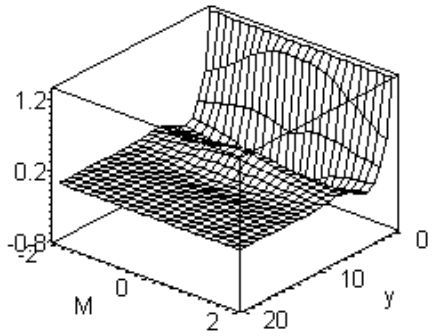

Fig. 2: Velocity distribution for various values of M

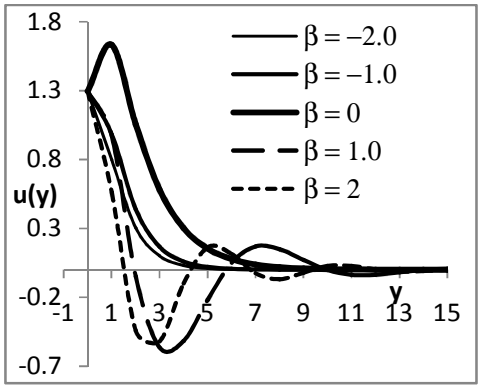

Fig. 3: Velocity distribution for various values of β

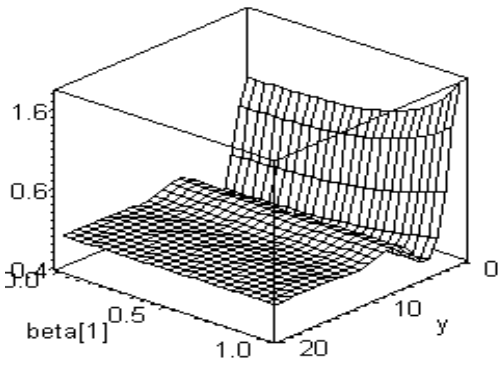

Fig.4: Velocity distribution for various values of β_1

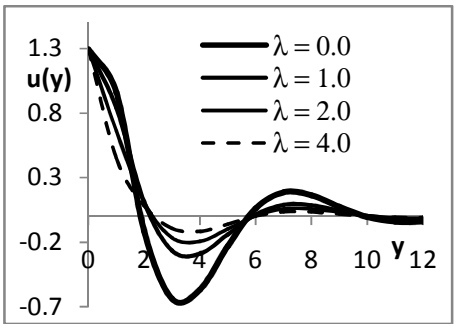

Fig. 5: Velocity distribution for various values of λ

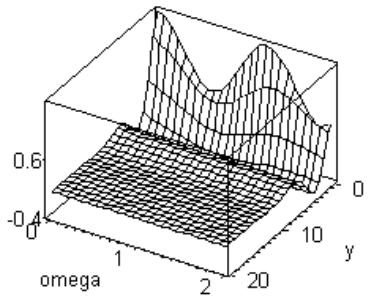

Fig. 6: Velocity distribution for various values of ω

Also the effect of MHD parameter (Hartmann number) on the velocity distribution is shown in Figure 2. We discovered that the maximum amplitude occurs when the Hartmann number is minimal. The effect of M on velocity is seen to stabilise the velocity as the maximum velocity only occur at the surface for higher values of *M*.

We show in Figure 3 the velocity distribution for different values of heat generation and/or absorption. We discovered that increase in heat generation increases the velocity of the flow. Meanwhile for heat absorption, the velocity decreases as heat absorption increases. While in Figure 4 we show that velocity increases as the acceleration of the plate increases. Figure 5 displayed the effect of porosity parameter on the velocity distribution. It could be seen that increases in porosity reduces the velocity amplitude, thus velocity distribution decreases as the porosity of the plate increases.

In Figure 6 we show the influence of oscillation frequency on the velocity profile. It could be seen that velocity oscillates alongside whit the plate. Effect of Prandtl number (Pr) on the velocity distribution is displayed in Figures 7 and 8. It is observed from both figures that temperature distribution decreases as the prandtl number increases. Moreover, we observed that for lower values of Prandtl number corresponding to mercury, temperature distribution is higher which validate the assertion that mercury conduct heat better than other species, hence the temperature is highest.

Figures 9 and 10 shows temperature distribution for different values of heat generation/absorption and acceleration respectively. Unlike the case of velocity distribution, we discovered from Figure 9 that increase in heat generation reduce the temperature of the flow. Meanwhile for heat absorption, the temperature amplitude decreases as heat absorption increases. While in Figure 10 we show that temperature increases as the acceleration of the plate increases with little amplitude. In Figure 11, it is shown that Hall parameter increases the velocity distribution until a steady state is attained after which little or no difference in the velocity profile is observed. This is shown in figure 11 by the clustering of the velocity curves as Hall parameter is sufficiently large.

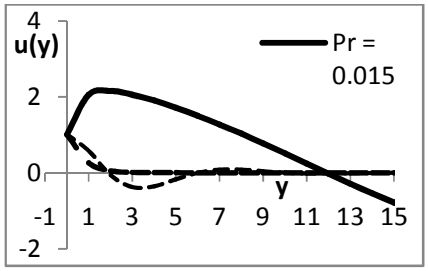

Fig. 7: Velocity distribution for various values of Prandtl number

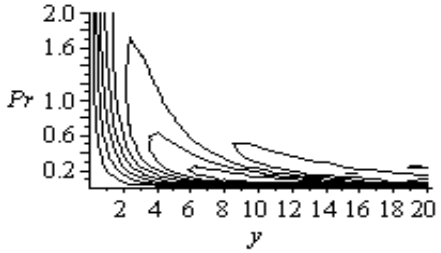

Fig. 8: Temperature distribution for Prandtl number against position y

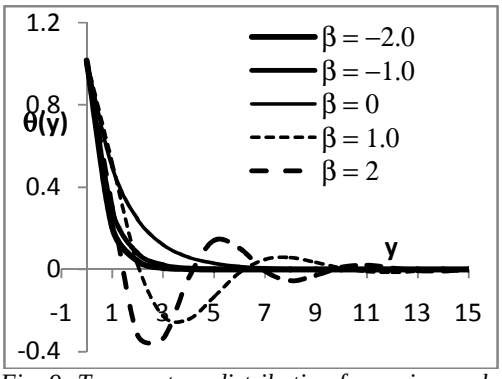

Fig. 9: Temperature distribution for various values of β

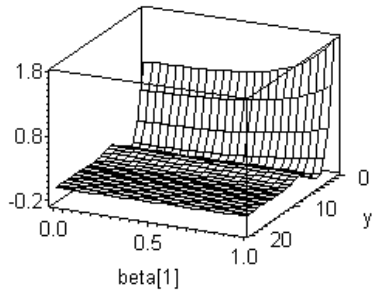

Fig. 10: Temperature distribution for various values of β

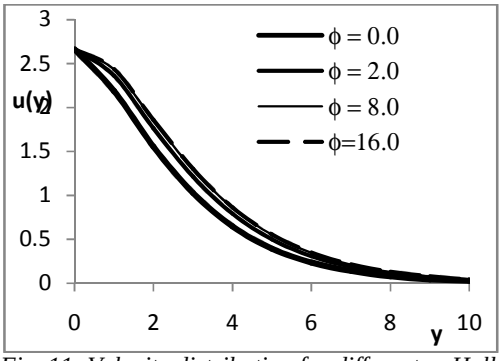

Fig. 11: Velocity distribution for different Hall Parameter

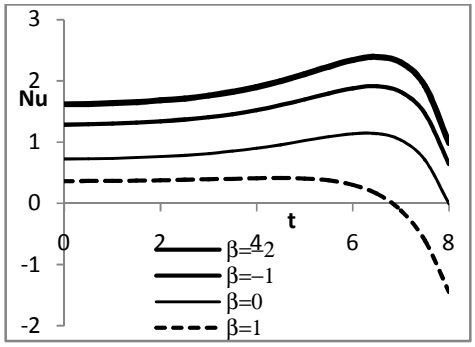

Fig. 12: Rate of heat transfer at the wall distribution for various values of β

Skin – friction and Heat flux.

The non-dimensional skin friction (C_f) and the heat flux in terms of Nusselt number (*Nu*) are shown in figures 12 – 18 for different values of heat generation/absorption, MHD parameter, Hall parameter and thermal Grashof number.

Figure 12 shows the effect of heat source/sink on rate of heat transfer at the wall. Comparing the curves in the figure, we could see that rate of heat transfer at the wall increase with heat generation and decrease with heat sink. In Figure 13, we discovered that for mercury (Pr = 0.015), the rate of heat transfer at the wall is minima compare to other species. In fact, it could be seen that rate of heat transfer at the wall increase as Prandtl number increase. It could then be remarked that Nusselt number increase as thermal conductivity reduces.

The effect of Hall parameter on the skin – friction coefficient is as shown in Figure 14. It could be seen that skin – friction coefficient increase as Hall parameter increase. Like in the velocity distribution (Figure 11), for larger values of Hall parameter, changes in ϕ as no significant canes in the values of skin – friction coefficient.

We displayed the effect of Prandtl number on the Skin – friction coefficient. It is seen that skin – friction coefficient increase as thermal conductivity increase. Hence Skin – friction coefficient is highest for Mercury (Pr = 0.015) and lowest for water (Pr = 7.0). Thus Skin – friction coefficient reduces as Prandtl number increase.

We show the effect of heat source/sink in figure 16. Unlike rate of heat transfer at the wall, skin – friction coefficient reduces with heat generation. Effects of Hartmann number and Thermal Grashof number on the Skin – Friction coefficient are shown in Figures 17 and 18 respectively. It could be seen from Figure 17 that Skin – Friction coefficient decrease as Hartmann number increase. Comparing the curves Figure 18, we observed that in the case of heating of the plate (Grt<0), Skin – Friction coefficient decrease as Grt increase and vice – versa for cooling of the plate (Grt>0)

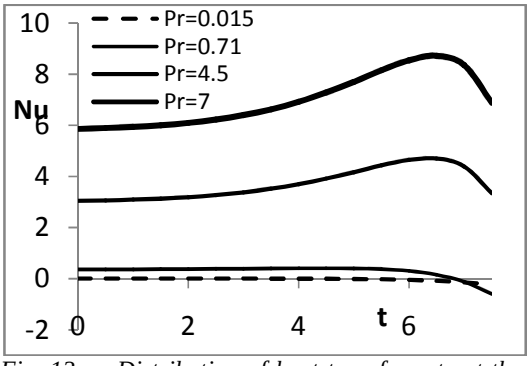

Fig. 13: Distribution of heat transfer rate at the wall for different Prandtl number

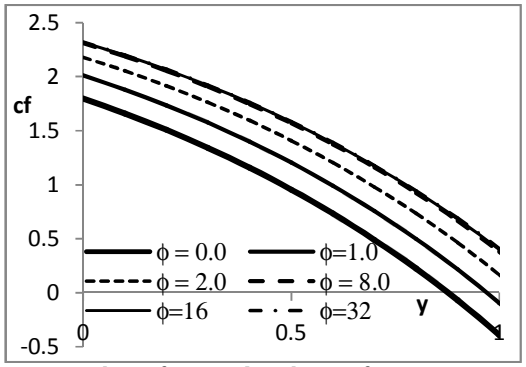

Fig. 14: Skin – friction distribution for various values of Hall Parameter

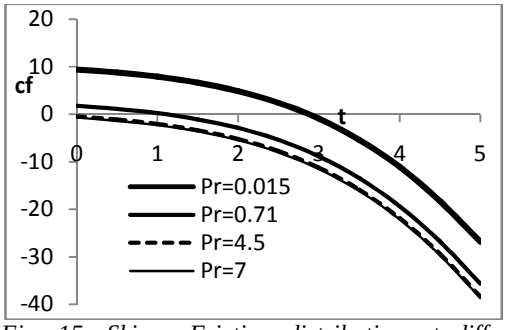

Fig. 15: Skin - Friction distribution at different values of Prandtl number

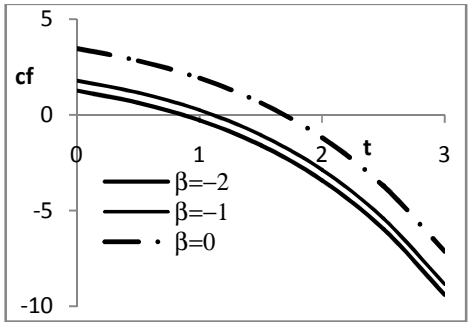

Fig. 16: Skin - Friction distribution at different values heat generation/absorption

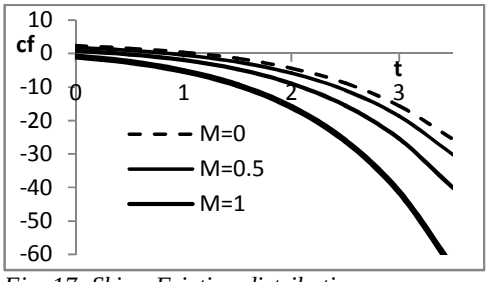

Fig. 17: Skin - Friction distribution at different values Hartmann number

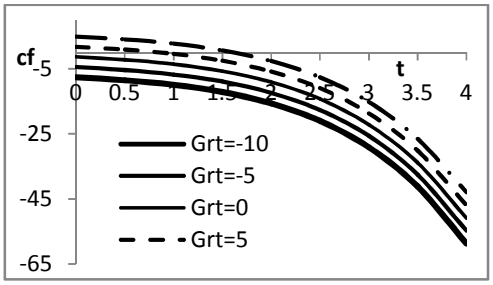

Fig. 18: Skin - Friction distribution at different values Grashof number

Concluding remarks

We have presented an exact solution for the unsteady motion of magnetohydrodynamic flow of oscillating plate in porous medium in presence of Hall current. The present analysis reveals the following conclusions:

- The Hartmann number has a pronounced effect on the velocity. With its increase the boundary layer increases and hence the velocity decreases. Similar effects are observed with the porosity parameter.
- Velocity amplitude is decreased with increase in Hall parameter and boundary layer thickness is increased with increase in Hall parameter.
- By increasing the strength of thermal Grashof number field, the velocity amplitude increaes.
- The amplitude of velocity becomes large in the case of deceleration and becomes smaller in the case of acceleration.

REFERENCES

[1] Crane L. J. 1970. *Flow past a stretching plate*. Zeit.angew. Math. Physik *21*, 645-647.

[2] Chakraborty A. and Gupta A. S. 1979. *Hydromagnetic flow and heat transfer over a stretching sheet.*Quart. Appl. Math. 37, 23 - 32.

[3] Dutta B. K. and Gupta A. S. 1989. *Cooling of a stretching sheet in viscous flow*. Ind. Eng. Chem. Research 26 (19~7) 333-336. DOI: 10.1021/ie00062a025.

[4] Navier C. L. 1827. *Me´moire sur les lois du mouvement des fluides*. Mem. Acad. Sci. Inst. France, Vol. 6, pp. 432-6.

[5] Davidson P.A. 2001. *An introduction to magnetohydrodynamics*. 1st Ed. Cambridge University ISBN-10: 0521794870 | ISBN-13: 978-0521794879

[6] Stokes G.G. 1901. *On the effect of the internal friction of fluids on the motion of pendulums.Transactions of the Cambridge Philosophical Society*, Vol. IX.p. [8] (1851); Math.and Phys. Papers, Cambridge, III, 1 – 141.

[7] Pop I., Kumari, M. and Nath G. 1994. *Conjugate MHD flow past a flat plate*, Acta Mechanica 106, 215 – 220. DOI: 10.1007/BF01213563. Online ISSN 1619-6937

[8] Wang C. Y. 1984. *The three-dimensional flow due to a stretching flat surface*. Physics of Fluids 27, 1915-1917. dx.doi.org/10.1063/1.864868

[9] Takhar H. S. Raptis A.A. and Perdikis C.P. 1987. *MHD asymmetric flow past a semi-infinite moving plate.* Acta Mech. 65, 287 – 290.

[10] Asghar S., Mohyuddin M.R., and Hayat T. 2005. *Effects of Hall current and heat transfer on flow due to a pull of eccentric rotating disks*. International Journal of Heat and Mass Transfer.48, 599-406. DOI:10.1016/j.ijheatmasstransfer.2004.08.023

[11] Guria M., Das S. and JanaR. N. (2007). Hall effects on unsteady flowof a viscous fluid due to non-coaxial rotation of a porous disk and a fluid at infinity. International Journal of Non-Linear Mechanics 42, 1204 – 1209 doi:10.1016/j.ijnonlinmec.2007.09.009

[12] Mohammadreza A, Davood Domiri Ganji, Farhad Abbassi, 2012. Study on MHD Viscous Flow over a Stretching Sheet Using DTM-Pade' Technique.*Modern Mechanical Engineering*, 2012, 2, 126-129 doi:10.4236/mme.2012.24016.

[13] Nield D.A. and A. Bejan A (1999). *Convection in porous media*, 2nd Ed. Springer, Berlin,.

[14] Cowling T. G. 1957. *Magnetohydrodynamics*.2nd Ed. London. Interscience Publishers Ltd, New York, p. 101.

[15] Sato H. 1961. *The Hall effects in the viscous flow of ionized gas between parallel plates under transverse magnetic field*. Journal of the Physical Society of Japan, Volume 16, Issue 7, 1427 – 1433.